

1 The Mexican Cavefish Mount a Rapid and Sustained Regenerative Response Following Skeletal
2 Muscle Injury

3
4 Luke Olsen^{1,2}, Huzaifa Hassan¹, Sarah Keaton³, Nicolas Rohner^{1,2*}

5
6 ¹Stowers Institute for Medical Research, Kansas City, MO 64110, USA

7 ²Department of Molecular & Integrative Physiology, University of Kansas Medical Center, Kansas City,
8 KS 66160, USA

9 ³Department of Biological Sciences, DePaul University, Chicago, IL 60614, USA

10

11 *Correspondence: Nicolas Rohner nro@stowers.org

12

13

14

15

16 Running Title: The Mexican Cavefish maintain the capacity to mount a rapid and sustained
17 immune system and stem cell response following localized skeletal muscle injury.

18

19 Keywords: Cavefish, Regeneration, Immune System, Inflammation, Stem Cell

20

21

22

23

24

25

26

27

28

29

30

31

32

33

34

35

36

37

38

39

40

41

42

43

44

45

46

47

48 **Summary**

49 Physical injury and tissue damage is prevalent throughout the animal kingdom, with the ability to
50 quickly and efficiently regenerate providing a selective advantage. The skeletal muscle possesses
51 a uniquely large regenerative capacity within most vertebrates, and has thus become an important
52 model for investigating cellular processes underpinning tissue regeneration. Following damage,
53 the skeletal muscle mounts a complex regenerative cascade centered around dedicated muscle stem
54 cells termed satellite cells. In non-injured muscle, satellite cells remain in a quiescent state,
55 expressing the canonical marker *Pax7* (Chen et al. 2020). However, following injury, satellite cells
56 exit quiescence, enter the cell cycle to initiate proliferation, asymmetrically divide, and in many
57 cases terminally differentiate into myoblasts, ultimately fusing with surrounding myoblasts and
58 pre-existing muscle fibers to resolve the regenerative process (Chen et al. 2020).

59
60 The innate immune system, specifically those of the myeloid lineage, are crucial for the sequential
61 steps described above (Tidball et al. 2017). For example, within the first few hours of muscle
62 damage, neutrophils and macrophages infiltrate the damaged skeletal muscle to mediate the repair
63 process; including phagocytosis of cellular debris, secretion of cytokines regulating satellite cell
64 dynamics, and temporal control of the pro- and anti-inflammatory phases (Tidball et al. 2010).
65 However, investment into the innate immune system is energetically costly resulting in many
66 species decreasing investment in the innate immune system under nutrient-limited environments
67 (McDade et al. 2016). Whether this reduced investment into the innate immune system results in
68 a decreased capacity to mount a regenerative response following tissue damage remains unclear.
69 To this point, we utilized the emerging evolutionary model, *Astyanax mexicanus*, to investigate
70 the consequence of shifts in immune system investment on skeletal muscle regeneration.

71
72 The *Astyanax mexicanus* is a single species, comprised of river-dwelling surface fish and cave-
73 dwelling cavefish. ~160,000 years ago, the ancestral surface fish colonized the surrounding caves
74 resulting in multiple independently derived cave populations (Herman et al. 2018). These caves
75 are completely devoid of light, resulting in diminished primary producers and a subsequent general
76 lack in biodiversity. These different selective pressures have led to many cave-specific
77 morphological and physiological adaptations (Krishnan et al. 2020; Stockdale et al. 2028; Peuß et
78 al. 2020; Olsen et al. 2022). For example, we found that the diminished macroparasite diversity in
79 certain caves affected the evolution of the immune investment strategy and the sensitivity of the
80 immune system towards immunological stimuli (e.g. lipopolysaccharides; LPS) of cavefish (Peuß
81 et al. 2020). Here, the hematopoietic niche of cavefish consists of less innate immune cells (e.g.,
82 neutrophils and monocytes) than the surface fish and we found that this reduction of
83 proinflammatory cells is compensated by a prolonged pro-inflammatory response through stronger
84 and more sustained expression of proinflammatory cytokines such as *il6*, *tnfa*, *illβ*, and *g-csf* upon
85 exposure to LPS (Peuß et al. 2020). Similarly, injuring the heart of *A. mexicanus* resulted in an
86 elevated immune response within cavefish relative to surface fish – a phenomenon thought to
87 underlie their inability to fully regenerate their cardiac tissue (Stockdale et al. 2018). To this point,
88 we sought to address whether a similar decrease in regenerative potential persists within the
89 cavefish skeletal muscle following injury via analyzing the transcriptional responses after
90 cardiotoxin injection in both surface fish and cavefish. The fact that cavefish and surface fish
91 populations are of the same species makes comparative transcriptomic approaches robust and
92 informative (Krishnan et al. 2020).

93 **Methods**

94 **Cardiotoxin injection and muscle collection**

95 All fish used were adult (1-2 years old) and reared at similar tank densities. Laboratory-reared
96 surface fish and cavefish (of the “Pachón” population) were fasted overnight and anesthetized in
97 ms222 for ~30 seconds or until movement stopped. Following anesthetization, fish were injected
98 with 0.3 mg/ml cardiotoxin dissolved in 1xPBS (pH 7.4). Control fish were similarly anesthetized
99 and injected with 1xPBS (pH 7.4). Injections were made immediately anterior to the dorsal fin to
100 decrease the likelihood of impacting swimming behavior. No obvious changes in swimming
101 behavior were observed. Following injection, fish were transferred to their tank water to regain
102 consciousness. Fish were then euthanized at 1 day post injury (dpi), 7dpi, and 14 dpi and skeletal
103 muscle was immediately dissected and frozen in liquid nitrogen. The timepoints utilized within
104 this study were determined based off previous literature and histological analysis of surface fish
105 skeletal muscle regeneration (Figure S2). Surface fish are considered as the ‘control’ group, and
106 we thus sought to determine the regenerative process first within surface fish and identify
107 timepoints which best reflect the central components of skeletal muscle regeneration (i.e. immune
108 cell infiltration and new muscle fiber formation). We determined timepoints ranging from 1dpi-
109 to-14dpi contained the most pertinent regenerative information and we thus used these timepoints
110 for our follow-up muscle collection from a separate cohort of surface fish and cavefish for
111 transcriptome analysis. All experiments and fish husbandry are approved under IACUC protocol
112 2021-129.

113 **RNA extraction and processing for RNA-sequencing**

114 ~100mg of frozen tissue was homogenized in 1mL Trizol (Ambion) with triple pure M-Bio grade
115 high impact zirconium beads in a Beadbug 6 microtube bead beater. RNA was extracted using

116 standard phenol/chloroform extraction. The RNA pellet was cleaned with the RNeasy Mini Kit
117 (Qiagen #74104) with on-column DNase digestion (Qiagen #79256). Libraries were prepared
118 according to the manufacturer's instructions using the TruSeq Stranded mRNA Prep Kit (Illumina
119 #20020594). The resulting libraries were quantified using a Bioanalyzer (Agilent Technologies)
120 and Qubit fluorometer (Life Technologies). Libraries were normalized, pooled, multiplexed, and
121 sequenced on an Illumina NextSeq-75-HO instrument as v2 Chemistry High Output 75bp single
122 read runs. Following sequencing, Raw reads were demultiplexed into Fastq format allowing up to
123 one mismatch using Illumina bcl2fastq2 (v2.20). Reads were aligned to the *Astyanax mexicanus*
124 reference genome from University of California Santa Cruz with STAR aligner (v 2.7.3a), using
125 Ensembl 102 gene models. Transcripts per million (TPM) values were generated using RSEM (v
126 1.3.0). Pairwise differential expression analysis was performed using Bioconductor package
127 edgeR (v3.24.3 with R v3.5.2). Only protein coding genes and long non-coding RNAs (lncRNAs)
128 were considered from the Ensembl 102 annotation. Only genes with counts per million expression
129 ≥ 0.5 in at least 2 samples were kept for further analyses. Statistical significance was determined
130 by fold change cutoff of 2 and false discovery rate (FDR) cutoff of 0.05 with the p.adjust function
131 in R with the default choice Benjamini & Hochberg correction. Spearman correlations between all
132 samples were determined and clustered. The correlation plot is based on the log₂ transformed
133 normalized gene expression values (TPM) that are generated using RSEM. The hierarchical
134 clustering heatmap includes genes expressed above 2 TPM in at least one sample and is clustered
135 based on Euclidean distance between samples. Gene Ontology (GO) Enrichment analysis was
136 performed on differentially expressed genes identified in edgeR using R package 'clusterProfile'.

137

138

139 **Results**

140 **Global gene expression response to skeletal muscle injury**

141 To characterize the regenerative response of *A. mexicanus*, we injected fish skeletal muscle with
142 the necrotic agent cardiotoxin – shown to result in rapid and dramatic muscle necrosis (Seger et
143 al. 2011 and Figure S2). Following injection, we collected skeletal muscle 1-day, 7-days, and 14-
144 days post injury (dpi) followed by genome-wide analysis via bulk RNA-sequencing (Fig. 1A). In
145 sum, we found cardiotoxin injection resulted in a more robust gene expression response at both
146 the 1dpi, 7dpi, and 14dpi timepoints within cavefish relative to surface fish. Specifically, we
147 identified 2,936 differentially expressed genes (DEG's) at 1dpi within cavefish which markedly
148 decreased to 944 DEG's at 7dpi, and 1,656 DEG's at 14dpi. Surface fish showed a similar, albeit
149 reduced, increase in DEG's at the 1dpi timepoint with a total of 1,851 DEG's identified. This
150 number decreased at 7dpi to 673 DEG's, and continued to decrease at 14dpi with no DEG's
151 detected. In support of this, hierarchical clustering revealed the 1dpi samples clustered more
152 distinctly than all other timepoints (Fig. 1B). Taken together, we find that cardiotoxin injection
153 results in a robust change in gene expression within both cavefish and surface fish skeletal muscle,
154 with a more extreme and sustained change in gene expression within cavefish.

155

156 **Immune response following skeletal muscle injury**

157 Because of our recent findings that cavefish have decreased investment in the innate branch of the
158 immune system – an essential component of muscle regeneration – we sought to explore gene
159 expression changes underlying pro- and anti-inflammatory signaling. We first conducted a Gene
160 Ontology enrichment analysis of all DEG's at each timepoint and, as expected, identified multiple
161 pathways enriched for the immune system. Specifically, we found “immune response” ($p=0.0014$),

162 “adaptive immune response” ($p=0.0016$), and “positive regulation of immune response” ($p=0.006$)
163 increased at 7dpi within surface fish (Fig. S1A). Cavefish showed a similar increase in immune-
164 related pathways, such as “immune response” ($p=0.0116$) and “defense response” ($p=0.0116$),
165 albeit at the 1dpi timepoint (Fig. S1B). As shown in Figure 1C, most genes within these pathways
166 increased following injection, most dramatically at 1dpi and 7dpi, and tended to decrease back to
167 baseline at 14dpi, though to a lesser degree in cavefish, a possible reflection of prolonged immune
168 signaling following muscle damage. In fact, when pooling all genes identified within the “immune
169 response” pathway, cavefish showed a greater increase in expression relative to surface fish (Fig.
170 1D).

171
172 In addition to those within the “immune response” pathway, we sought to characterize classical
173 markers regulating inflammation previously shown to be differentially regulated between cavefish
174 and surface fish, specifically the cytokines *il6*, *tnfa*, *il1 β* , and *g-csf* (*gcsfa*). In agreement with our
175 previous findings, cavefish had reduced basal expression relative to surface fish. Interestingly
176 however, cavefish showed a robust increase in expression at 1dpi, having an ~19-fold, 37-fold, 9-
177 fold, and 6-fold increase in expression of *il6*, *tnfa*, *il1 β* , and *g-csf*, respectively, relative to an ~4-
178 fold, 5-fold, 2-fold, and 1.1-fold increase, respectively, within surface fish (Fig. S1C). These data
179 support our previous findings of cavefish having fewer innate immune cells (indicated by
180 decreased expression at baseline), however, having heightened sensitivity following an
181 inflammatory stimulus relative to surface fish – at least within the local site of injection (Peuß et
182 al. 2020).

183

184

185 **Cavefish have an increased satellite cell response to injury**

186 The ability to efficiently coordinate the inflammatory response following muscle injury is critical
187 for functional satellite cell dynamics and the resolution of regeneration. Because cavefish appear
188 to possess a more robust inflammatory response relative to surface fish following cardiotoxin
189 injection, we sought to determine how this influences satellite cell dynamics, specifically the
190 central genes regulating satellite cell quiescence (*pax7a/b*), activation/proliferation (*myf5/myod*),
191 differentiation (*myod/myog*), and ultimate myoblast fusion (*mymk*) (Chen et al. 2020; Millay et al.
192 2013). As expected, many of these genes were increased in expression within both surface fish and
193 cavefish following cardiotoxin injection. Surprisingly though, cavefish showed a more robust and
194 sustained increase in expression relative to surface fish. For example, cavefish had a significant
195 increase in *pax7b* at the 7dpi and 14dpi timepoint whereas surface fish increased but did not reach
196 statistical significance (Fig. 1E). Additionally, cavefish increased expression of *myf5* (at 7 and
197 14dpi) and *myog* (at 1, 7, and 14dpi) following injury whereas surface fish only increased *myog* at
198 7dpi (Fig. 1E). Moreover, *mymk* showed a robust increase at the 7dpi and 14dpi timepoints within
199 cavefish while increasing only at the 7dpi timepoint within surface fish. As such, in agreement
200 with the immune system dataset, cavefish showed a more robust and sustained increase in genes
201 orchestrating satellite cell dynamics following injury, a possible reflection of their heightened
202 sensitivity to an external stimulus.

203

204 **Discussion**

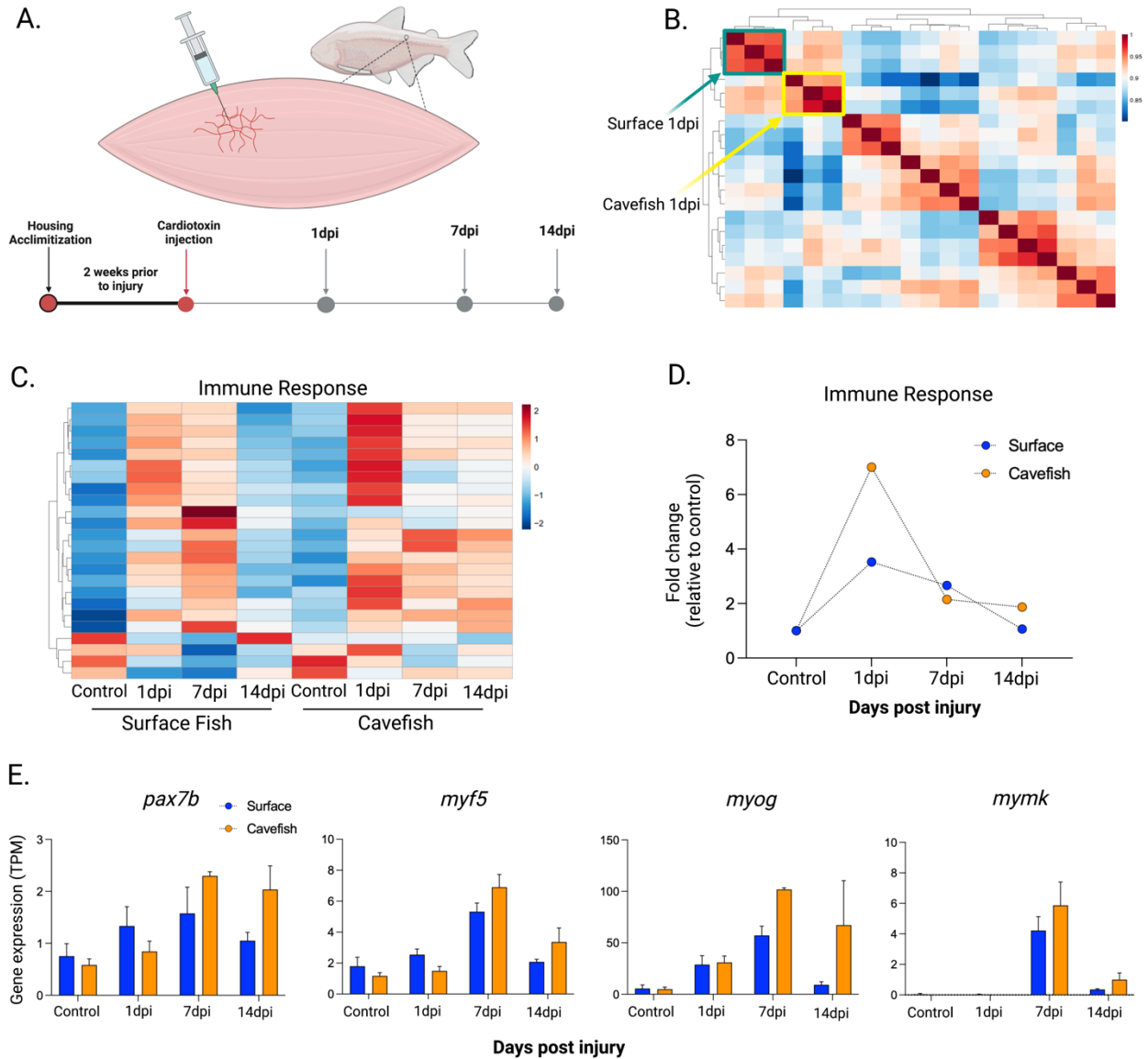
205 Here we provide evidence suggesting cavefish skeletal muscle initiates a ‘hyper-sensitive’
206 inflammatory response following local muscle injury. We reasoned this may result in
207 dysregulation of the satellite cell response – similar to what is seen following cardiac injury within

208 cavefish – but, in contrast to our expectations, cavefish demonstrated a more robust increase of
209 markers regulating satellite cell proliferation, differentiation, and fusion when compared to surface
210 fish. This may reflect cavefish being more sensitive to an injury stimulus and thus requiring a
211 greater reliance on their satellite cell pool as compared to surface fish. While these data provide
212 the necessary first step in delineating cavefish skeletal muscle regeneration, future work is required
213 to confirm that our observations at the level of gene expression are in fact consequential toward
214 muscle regeneration. For example, the sustained immune response seen within the cardiac tissue
215 of cavefish results in scarring and fibrosis, a possible result within cavefish skeletal muscle. As
216 such, histological analysis of cavefish and surface fish skeletal muscle at multiple timepoints
217 following injury is required to determine whether our findings indicate a physiological or
218 pathological response to muscle injury.

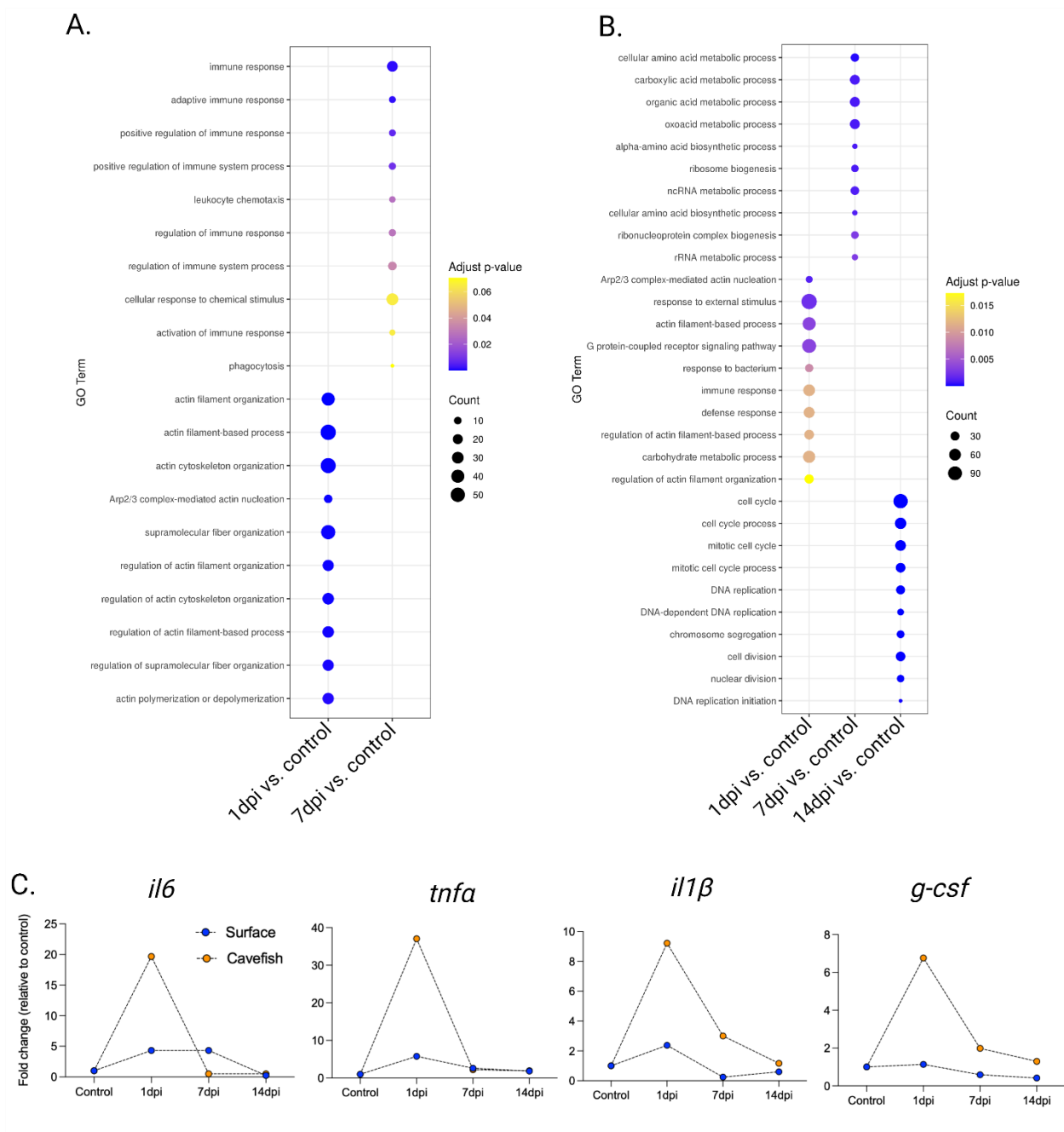
219

220 **Acknowledgements**

221 We would like to thank the cavefish facility at the Stowers Institute for cavefish husbandry support,
222 specifically Molly Miller, Elizabeth Fritz, David Jewell, Andrew Ingalls, Zachary Zakibe, Cole
223 Biesemeyer, Hailey Gregory, and Diana Baumann. We thank Mark Miller for assistance with
224 illustrations. We thank all core support provided by the Stowers Institute; specifically, Rhonda
225 Egidy and Amanda Lawlor of Sequencing and Discovery Genomics. We would like to thank
226 Robert Peuß for the critical review of our manuscript. NR is supported by institutional funding,
227 NIH Grant 1DP2AG071466-01, NIH Grant R01 GM127872, NSF IOS-1933428, and NSF EDGE
228 award 1923372.

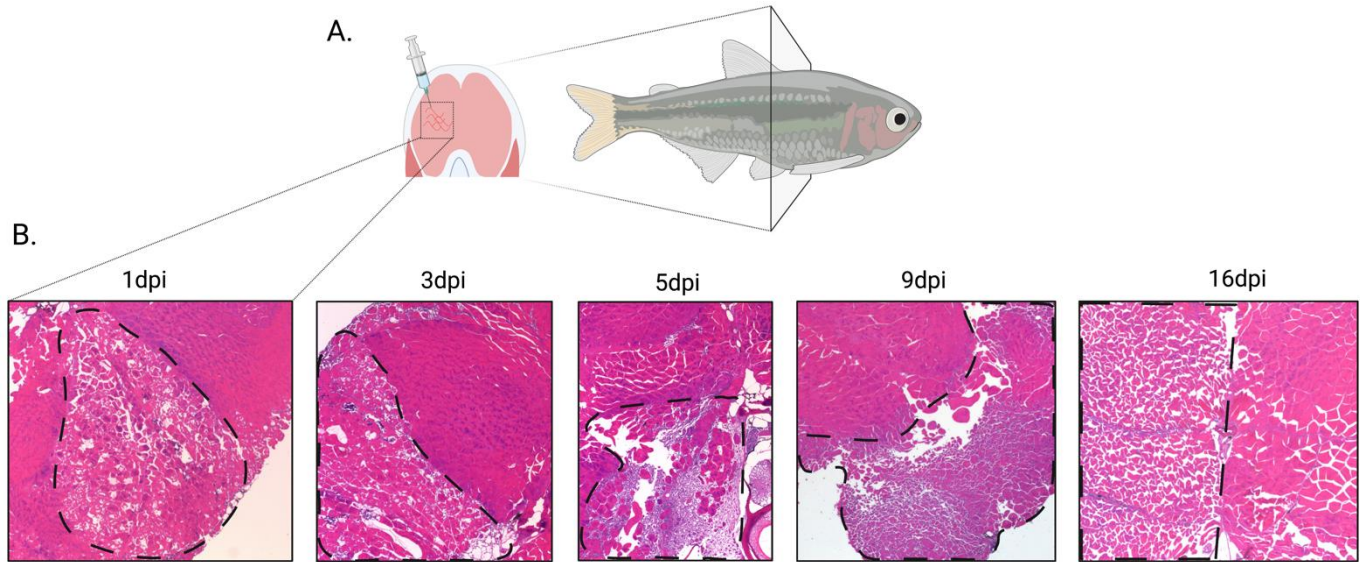


229 **Figure 1.** (A) Schematic of cardiotoxin injection and tissue collection at 1 day post injury (dpi), 7dpi, and
 230 14dpi. (B) Hierarchical clustering heatmap of each sample analyzed with specific emphasis placed on 1dpi
 231 in both surface fish (green) and cavefish (yellow). (C) Heatmap of the genes identified within the immune
 232 response pathway of surface fish at the 7dpi timepoint and the corresponding genes within cavefish. (D)
 233 Average fold change of the genes identified within the immune response pathway (from Fig. 1C). (E)
 234 Relative gene expression of canonical satellite cell markers in transcripts per million (TPM).



235 **Figure S1.** Gene Ontology enrichment analysis of the differentially expressed genes from 1dpi, 7dpi, and
 236 14dpi relative to control (not injected) from (A) surface fish and (B) cavefish. Surface fish (Fig. S1A) did
 237 not have any DEG's at the 14dpi timepoint relative to control. (C) Fold change of the pro-inflammatory
 238 cytokines *il6*, *tnfa*, *il1β*, and *g-csf*. Each timepoint is the mean of two-to-three biological replicates.

239
 240
 241
 242



243 **Figure S2.** (A) Schematic of the site of skeletal muscle injection. (B) Representative images of muscle
244 collected from the injured tissue at 1 day post injury (dpi), 3dpi, 5dpi, 9dpi, and 16dpi to determine the
245 timepoint for the transcriptome analysis. The site of injury is demarcated by the black dashed line with the
246 non-injured muscle directly adjacent. As mentioned within the Methods section, surface fish served as the
247 control, and we thus determined the necessary timepoints for muscle collection of both cavefish and surface
248 fish following histological analysis from surface fish at multiple timepoints post injury (shown above). As
249 such, all images are from surface fish.

250
251
252
253
254
255
256
257
258
259
260
261
262
263
264
265

266 **References**

267 Chen, W., Datzkiw, D., & Rudnicki, M. A. (2020). Satellite cells in ageing: use it or lose it. *Open*
268 *biology*, 10(5), 200048.

269
270 Tidball, J. G., & Villalta, S. A. (2010). Regulatory interactions between muscle and the immune system
271 during muscle regeneration. *American journal of physiology. Regulatory, integrative and comparative*
272 *physiology*, 298(5), R1173–R1187.

273
274 Tidball J. G. (2017). Regulation of muscle growth and regeneration by the immune system. *Nature reviews.*
275 *Immunology*, 17(3), 165–178.

276
277 Krishnan, J., Persons, J. L., Peuß, R., Hassan, H., Kenzior, A., Xiong, S., Olsen, L., Maldonado, E.,
278 Kowalko, J. E., & Rohner, N. (2020). Comparative transcriptome analysis of wild and lab populations of
279 *Astyanax mexicanus* uncovers differential effects of environment and morphotype on gene
280 expression. *Journal of experimental zoology. Part B, Molecular and developmental evolution*, 334(7-8),
281 530–539.

282
283 McDade, T. W., Georgiev, A. V., & Kuzawa, C. W. (2016). Trade-offs between acquired and innate
284 immune defenses in humans. *Evolution, medicine, and public health*, 2016(1), 1–16.

285
286 Millay, D. P., O'Rourke, J. R., Sutherland, L. B., Bezprozvannaya, S., Shelton, J. M., Bassel-Duby, R., &
287 Olson, E. N. (2013). Myomaker is a membrane activator of myoblast fusion and muscle
288 formation. *Nature*, 499(7458), 301–305.

289
290 Olsen, L., Levy, M., Medley, J. K., Hassan, H., Alexander, R., Wilcock, E., . . . Rohner, N. (2022). Metabolic
291 reprogramming underlies cavefish muscular endurance despite loss of muscle mass and contractility. *bioRxiv*,
292 2022.2003.2012.484091.

293
294 Peuß, R., Box, A. C., Chen, S., Wang, Y., Tsuchiya, D., Persons, J. L., Kenzior, A., Maldonado, E.,
295 Krishnan, J., Scharsack, J. P., Slaughter, B. D., & Rohner, N. (2020). Adaptation to low parasite abundance
296 affects immune investment and immunopathological responses of cavefish. *Nature ecology &*
297 *evolution*, 4(10), 1416–1430.

298

- 299 Seger, C., Hargrave, M., Wang, X., Chai, R. J., Elworthy, S., & Ingham, P. W. (2011). Analysis of Pax7
300 expressing myogenic cells in zebrafish muscle development, injury, and models of disease. *Developmental*
301 *dynamics: an official publication of the American Association of Anatomists*, 240(11), 2440–2451.
302
- 303 Stockdale, W. T., Lemieux, M. E., Killen, A. C., Zhao, J., Hu, Z., Riepsaame, J., Hamilton, N., Kudoh, T.,
304 Riley, P. R., van Aerle, R., Yamamoto, Y., & Mommersteeg, M. T. M. (2018). Heart Regeneration in the
305 Mexican Cavefish. *Cell reports*, 25(8), 1997–2007.e7.
306
- 307 Herman, A., Brandvain, Y., Weagley, J., Jeffery, W. R., Keene, A. C., Kono, T. J. Y., . . . McGaugh, S. E.
308 (2018). The role of gene flow in rapid and repeated evolution of cave-related traits in Mexican tetra,
309 *Astyanax mexicanus*. *Mol Ecol*, 27(22), 4397-4416.